

Chitosan/poly(2-ethyl-2-oxazoline) films for ocular drug delivery: Formulation, miscibility, in vitro and in vivo studies

Article

Accepted Version

Abilova, G. K., Kaldybekov, D. B., Ozhmukhametova, E. K., Saimova, A. Z., Kazybayeva, D. S., Irmukhametova, G. S. and Khutoryanskiy, V. V. ORCID: <https://orcid.org/0000-0002-7221-2630> (2019) Chitosan/poly(2-ethyl-2-oxazoline) films for ocular drug delivery: Formulation, miscibility, in vitro and in vivo studies. *European Polymer Journal*, 116. pp. 311-320. ISSN 0014-3057 doi: 10.1016/j.eurpolymj.2019.04.016 Available at <https://centaur.reading.ac.uk/83324/>

It is advisable to refer to the publisher's version if you intend to cite from the work. See [Guidance on citing](#).

Published version at: <https://www.sciencedirect.com/science/article/pii/S0014305719303313>

To link to this article DOI: <http://dx.doi.org/10.1016/j.eurpolymj.2019.04.016>

Publisher: Elsevier

All outputs in CentAUR are protected by Intellectual Property Rights law, including copyright law. Copyright and IPR is retained by the creators or other copyright holders. Terms and conditions for use of this material are defined in the [End User Agreement](#).

www.reading.ac.uk/centaur

CentAUR

Central Archive at the University of Reading

Reading's research outputs online

**Chitosan/poly(2-ethyl-2-oxazoline) films for ocular drug delivery:
formulation, miscibility, *in vitro* and *in vivo* studies**

Guzel K. Abilova,^a Daulet B. Kaldybekov,^{a,b} Elvira K. Ozhmukhametova,^c Aisulu Zh. Saimova,^c
Diara S. Kazybayeva,^a Galiya S. Irmukhametova,^a Vitaliy V. Khutoryanskiy^{b,*}

^a *Department of Chemistry and Chemical Technology, Al-Farabi Kazakh National University,
050040 Almaty, Kazakhstan*

^b *School of Pharmacy, University of Reading, Whiteknights, RG6 6AD Reading, United Kingdom*

^c *Semey State Medical University, 071400 Semey, Kazakhstan*

***Corresponding author:**

Postal address: School of Pharmacy, University of Reading, Whiteknights, PO Box 224, RG6 6AD
Reading, United Kingdom

E-mail address: v.khutoryanskiy@reading.ac.uk

Telephone: +44(0) 118 378 6119

Fax: +44(0) 118 378 4703

20 **ABSTRACT**

21 Polymeric films were prepared based on chitosan and its blends with poly(2-ethyl-2-oxazoline)
22 by casting from aqueous solutions. These materials were characterised using a number of
23 physicochemical techniques, including Fourier-transform infrared spectroscopy, thermal gravimetric
24 analysis, differential scanning calorimetry, wide angle x-ray diffraction, tensile testing and scanning
25 electron microscopy. All these studies indicate that there is a weak intermacromolecular hydrogen
26 bonding between these polymers, which facilitates their complete miscibility in solid state. These
27 films were formulated with sodium fluorescein as a model drug and were evaluated for their potential
28 application in ocular drug delivery both *in vitro* and *in vivo*. It was established that the films are
29 biocompatible and mucoadhesive; they are capable of providing a sustained drug release when
30 administered topically on the cornea.

31 **Keywords:** *chitosan, poly(2-oxazoline), films, miscibility, mucoadhesion, ocular drug delivery*

32 **1. INTRODUCTION**

33 Ability of hydrophilic polymers to stick to wet surfaces in the human body, defined as
34 mucoadhesion, has been widely used for designing dosage forms for transmucosal administration.
35 The current applications of mucoadhesive dosage forms include drug delivery to the eye, nose, oral
36 cavity, gastrointestinal tract, vagina, rectum and urinary bladder [1–5]. These routes of drug
37 administration offer a number of advantages and the use of mucoadhesive carriers facilitates better
38 dosage form retention on mucosal surfaces resulting in improved drug bioavailability, possibility of
39 targeting particular organs, ease of application and avoidance of painful injections.

40 Typically, all water-soluble polymers have some mucoadhesive properties; however, either
41 positively or negatively charged polyelectrolytes exhibit better ability to stick to mucosal tissues
42 compared to non-ionic macromolecules [2]. Chitosan as a polysaccharide of cationic nature is
43 considered as one of the materials with excellent mucoadhesive properties and its numerous

44 applications in transmucosal drug delivery have been demonstrated [6–8]. Many attempts have been
45 reported to modify mucoadhesive properties of chitosan through its chemical modification, as
46 discussed in a recent review by Ways et al [9]. Additionally, properties of chitosan could also be
47 altered by simple blending with other polymers. For example, Luo et al [10] demonstrated that
48 chitosan forms miscible blends with hydroxyethylcellulose, which resulted in reduction of
49 mucoadhesive properties of the buccal films based on the mixtures of these polymers. Freag et al [11]
50 reported the development of mucoadhesive sponges based on blends of chitosan with
51 hydroxypropylmethylcellulose and demonstrated that the materials prepared from 1:1 polymer
52 mixture exhibited the best physicochemical characteristics suitable for buccal administration. Sizílio
53 et al [12] fabricated mucoadhesive films by blending chitosan with poly(N-vinyl pyrrolidone) and
54 evaluated their application for delivery of betamethasone-17-valerate used in the therapy of recurrent
55 aphthous stomatitis.

56 Poly(2-oxazolines) is an emerging class of polymers highly promising for biomedical
57 applications due to their non-toxicity, bio-inert nature and unique physicochemical properties [13–
58 17]. Water-soluble representatives of this class such as poly(2-methyl-2-oxazoline), poly(2-ethyl-2-
59 oxazoline), and poly(N-propyl-2-oxazoline) have received a lot of attention of researchers due to their
60 unique physicochemical properties such as the ability to form hydrogen-bonded complexes with
61 polycarboxylic acids and tannins [18–20] as well as their temperature-responsive properties [21]. Due
62 to their bio-inert nature, low molecular weight poly(2-methyl-2-oxazoline) and poly(2-ethyl-2-
63 oxazoline) (5 kDa) were reported to facilitate mucus-penetration of silica nanoparticles through
64 porcine stomach mucosa [22,23] and to reduce their mucoadhesion to rat intestinal tissues [24].
65 Poly(2-ethyl-2-oxazolines) with larger molecular weights (50, 200 and 500 kDa) exhibited weak
66 mucoadhesive properties and their simple blends and complexes with Carbopols 971 and 974 also
67 resulted in reduction of dosage forms mucoadhesiveness compared to pure Carbopols® [25].

68 Polymer blending and miscibility of poly(2-oxazolines) with other polymers is studied
69 insufficiently. Earlier publications reported the miscibility studies of poly(2-oxazolines) with

70 hydroxyl-containing polymers [26–28] and some conventional plastic materials such as poly(vinyl
71 chloride), polystyrene, polypropylene and poly(vinylidene fluoride) [29]. Despite the growing
72 biomedical importance of both chitosan and poly(2-oxazolines) the studies of miscibility in their
73 blends are limited only to a very few publications [30].

74 In the present work we have prepared chitosan/poly(2-ethyl-2-oxazoline) films by casting from
75 aqueous mixtures of these polymers; studied the physicochemical properties of these blends using
76 Fourier transform infrared spectroscopy, thermal analysis and X-ray diffraction methods, tensile
77 properties, and scanning electron microscopy; and evaluated the mucoadhesive potential and
78 retention of these films on freshly excised bovine cornea *ex vivo* and on rabbit ocular cornea *in vivo*.

79 **2. EXPERIMENTAL SECTION**

80 **2.1. Materials**

81 A high molecular weight chitosan (CHI, $M_w \sim 310 - 375$ kDa, degree of deacetylation: 75 –
82 85%), poly(2-ethyl-2-oxazoline) (POZ, $M_w \sim 50$ kDa and PDI 3 – 4), hydrochloric acid solution
83 (HCl, 1 M), fluorescein sodium salt (NaFl) and phosphate buffered saline (PBS) tablets were
84 purchased from Sigma-Aldrich (Gillingham, UK). All other chemicals were of analytical grade and
85 used without further purification.

86 **2.2. Preparation of films**

87 Chitosan solution was prepared by first dissolving 3.75 g of chitosan in 25 mL of 1 M HCl,
88 then the total volume was made up to 500 mL with deionised water (CHI 0.75% w/v, pH ~ 4.0) and
89 stirred magnetically overnight at room temperature. Before casting CHI solution was sonicated in a
90 sonication bath (FS200b, Decon Laboratories Ltd., UK) for 30 min. Poly(2-ethyl-2-oxazoline)
91 solutions (0.75% w/v) were prepared by dissolving 3.75 g polymer powder in 500 mL of deionised
92 water (pH ~ 6.8) for 1 h under continuous stirring. The film-forming solutions (FFS) with and without
93 NaFl (0.1 mg/mL) were obtained by mixing CHI and POZ aqueous solutions at different volume
94 ratios, where part of CHI was gradually replaced with POZ, up to 60%. Formulations were named

95 indicating the CHI/POZ volume ratio as CHI (100), (80:20), (60:40), (40:60) and POZ (100),
96 respectively. The pH values of combined solutions were in the range of 4.0 – 4.2. FFS were
97 magnetically stirred for 3 h until fully homogeneous mixture formed, after that, 45 mL of each
98 solution was poured into 90 mm diameter Petri dishes and dried at room temperature for several days.

99 **2.3. Fourier transform infrared (FTIR) spectroscopy**

100 FTIR spectra were recorded on Nicolet iS5 FTIR spectrometer (Thermo Scientific, UK) using
101 an attenuated total reflectance (ATR) accessory equipped with a diamond crystal. The transmission
102 mode was used and the resolution was 1 cm⁻¹.

103 **2.4. Thermogravimetric analysis (TGA)**

104 Thermogravimetric analysis of CHI, POZ and CHI/POZ blend film samples was conducted
105 using Q50 TGA analyser (TA Instruments, UK) in the range between 20 and 600 °C at a heating rate
106 of 10 °C/min under nitrogen atmosphere. Moisture content in each film was determined from the
107 weight loss corresponding to the first step weight loss in their TGA curves (up to about 150 °C).

108 **2.5. Differential scanning calorimetry (DSC)**

109 Differential scanning calorimetry (DSC) measurements were performed on TA-Q2000 DSC
110 instrument (TA Instruments, UK). DSC thermograms of each film were recorded from the second
111 heating run at 20 °C/min, after the first run of heating up to 80 °C and cooling down to 25 °C at 10
112 °C/min, under nitrogen atmosphere, in order to estimate the glass transition temperatures (T_g).

113 **2.6. X-Ray diffraction (XRD)**

114 X-Ray diffraction patterns of the polymers and their blends were evaluated using Oxford
115 Diffraction Gemini Ultra diffractometer fitted with CuK α radiation and Saturn detector (Oxford
116 Diffraction Ltd., UK). Film samples were cut in 1×1 cm, loaded, and scanned at diffraction ranges
117 from 6 to 120° with a scan step of 0.01°, generating characteristic diffractograms at the rate of 2.5
118 scans min⁻¹.

119 **2.7. Scanning electron microscope (SEM)**

120 SEM experiments used a FEI Quanta 600 FEG Environmental Scanning Electron Microscope
121 instrument (FEI UK Ltd., UK) with an acceleration voltage of 20 kV. The images were taken from
122 the fracture surface of the materials, which were preliminary frozen in liquid nitrogen and coated with
123 gold sputter to facilitate high resolution imaging.

124 **2.8. Mechanical analysis**

125 Puncture strength (PS) and elongation at break (EB) of the films were measured using a TA.XT
126 Plus Texture Analyser (Stable Micro Systems Ltd., UK) in compression mode at room temperature
127 [31,32]. Film thickness was measured with a hand-held micrometer; six replicates were taken for each
128 sample in different places and the mean values were calculated accordingly. The thickness of the
129 films was about 0.065 ± 0.002 mm. The square shaped film samples (30 x 30 mm) fixed by screws
130 between two plates with a cylindrical hole of 10 mm diameter (area of the sample holder hole: $Ar_s =$
131 78.54 mm^2) and compressed by the upper load 5 mm stainless steel spherical ball probe (P/5S) at a
132 test speed 1.0 mm/sec. The plate was stabilised to avoid movements using two pins. The
133 measurements started after the probe was in contact with the sample surface. The probe moved at a
134 constant speed until each film sample was broken [33]. These tests were performed with the following
135 settings: pre-speed test 2.0 mm/sec; test-speed 1.0 mm/sec; post-test speed 10.0 mm/sec; target mode
136 – distance; distance 5 mm; trigger type auto; trigger force 0.049 N. The film samples were punctured
137 and the force required in Newtons was recorded and puncture strength was calculated using the
138 following equation [33,34]:

$$139 \qquad PS = \frac{\text{Force}}{Ar_s} \qquad (1)$$

140 where Force is the maximum applied force recorded during strain.

141 Elongation at break (EB) is the ratio between the extension of the film at the point of rupture
142 and the initial length of the sample and is expressed in percentage:

$$EB = \left(\frac{\sqrt{a'^2 + b^2} + r}{a} - 1 \right) \times 100\% \quad (2)$$

where a' – the initial length of the film sample that is not punctured by the probe; b – the penetration depth/vertical displacement by the probe; r – the radius of the probe; and a – radius of the film in the sample holder opening.

All experiments were conducted 5 times and the mean values \pm standard deviations were calculated and evaluated statistically.

2.9. *Ex vivo* mucoadhesion studies on bovine cornea

The retention of polymeric films on bovine eyes was studied using the protocols previously reported by our group with some modifications [35,36]. The bovine eyes are commonly used in ocular drug delivery and irritation testing because of their availability, suitable dimensions and structural similarity to human eyes [37]. These were acquired from P.C. Turner Abattoirs (Farnborough, UK) immediately after animal slaughter and were transported to the laboratory in a cold polystyrene container. Bovine corneas were dissected within 4 h of eyes delivery, where the whole cornea with 2-3 mm of sclera was carefully excised using a sharp blade. Each cornea was rinsed with PBS solution, placed in Petri dishes, wrapped with cling film to reduce dehydration and stored at 4 °C to be used on the following day. Each experiment was performed in triplicate using different corneas.

Experiments were carried out with a cornea mounted on a glass slide placed on half cut falcon tubes already mounted at an angle of 45° and maintained at 37 °C in an incubator. Prior to each experiment, spherically shaped polymeric discs (4 mm in diameter) containing NaFl were quickly soaked in 0.9% NaCl saline solution (1 sec) and then placed on cornea previously rinsed with 1 mL of simulated tear fluid (STF: 3.35 g NaCl; 1 g NaHCO₃; and 0.0305 g CaCl₂ made up to 500 mL with deionised water). The background microscopy images were recorded for each cornea prior to administration of a fluorescent film. Then 12 mL of STF solution was dripped for 1 h on a corneal surface at a flow rate of 200 µL/min using a syringe pump. Fluorescence microscopy images of whole tissue were recorded after each wash every 5 min using a Leica MZ10F stereo-microscope (Leica

168 Microsystems, UK) with Leica DFC3000G digital camera at 0.8× magnification and 20 ms exposure
169 time (gain 3.0×), fitted with a GFP filter (blue, $\lambda_{\text{emission}} = 512$ nm). The microscopy images were then
170 analysed with ImageJ software by measuring the fluorescence pixel intensity after each washing
171 cycle. The pixel intensity of the blank samples (corneal mucosa without a fluorescent film) was
172 deducted from each measurement and data were normalised and converted into fluorescent intensity
173 values using the following equation:

$$174 \quad \text{Fluorescence intensity} = \frac{I - I_b}{I_0 - I_b} \times 100\% \quad (4)$$

175 where I is the fluorescence intensity of a given tissue sample with a mucoadhesive film after each
176 washing; I_b is the background fluorescence intensity of that tissue sample (a blank sample); and I_0 is
177 the initial fluorescence intensity of that sample (a tissue sample with mucoadhesive film on it prior
178 to the start of first washing).

179 In parallel, STF solution flowing through the corneal epithelium was collected at pre-
180 determined time points and used for determination of the percentage of NaFl washed off the corneal
181 surface. All the collected samples were diluted with STF, making up the total volume to 30 mL. The
182 amount of NaFl in each sample was then quantified using a FP-6200 spectrofluorometer (Jasco, UK)
183 at $\lambda_{\text{excitation}}$ and $\lambda_{\text{emission}}$ wavelengths of 460 and 512 nm, respectively. A standard curve used to
184 determine the amount of NaFl released from the films can be found in Supplementary information
185 (Figure S1).

186 All measurements were conducted in triplicate and the mean values \pm standard deviations were
187 calculated and evaluated statistically.

188 **2.10. *In vivo* experiments**

189 *In vivo* experiments on ocular administration of fluorescent films (CHI and CHI/POZ) were
190 conducted using chinchilla rabbits (2.5 – 4.0 kg) according to a previously described protocol [38].
191 These experiments were approved by Semey State Medical University (Kazakhstan) ethics committee

192 and were conducted following the ARVO Statement for the Use of Animals in Ophthalmic and Visual
193 Research. Before the start of experiments, rabbits were housed in standard cages and allowed free
194 access to food and water. In the beginning of each experiment rabbits were sedated with 0.2 mL (100
195 mg/mL) sodium thiopental (Arterium Corporation, Ukraine), previously dissolved in 10 mL of 0.9%
196 NaCl saline solution, administered through the lateral auricular vein. Approximately 5 min after
197 administration of sodium thiopental, polymeric discs containing NaFl (10 mm in diameter) were
198 quickly soaked (1 sec) in a saline solution (0.9% NaCl) and carefully placed on rabbit left eye's
199 cornea; their right eye always served as a control. The behaviour of each polymeric disc on the eye
200 was controlled visually and images were taken at different time intervals with a high resolution digital
201 camera. In addition, a weak UV light from an UVGL-25 Compact UV handheld lamp (Ultra-Violet
202 Products, UK) was shone into the eye to facilitate the detection of fluorescence.

203 Each type of polymeric film was tested in 3 rabbits and each experiment was conducted until a
204 film was detached or dislodged. The mean residence time values \pm standard deviations were
205 calculated and assessed for statistical differences.

206 **2.11. Statistical analysis**

207 Data acquired during these experiments, i.e. mean values \pm standard deviations were calculated
208 and assessed for significance using two-tailed Student's *t*-test and a one-way analysis of variance
209 (ANOVA) followed by Bonferoni *post hoc* test using GraphPad Prism statistical analysis software
210 (version 7.0; GraphPad Software Inc.), where $p < 0.05$ was considered as statistically significant.

211 **3. RESULTS AND DISCUSSION**

212 **3.1. Preparation and characterisation of films**

213 CHI and CHI/POZ blend films were successfully developed and tested. These two polymers
214 are well characterised for their safety and biocompatibility and known to be stable under normal
215 processing and storage conditions. POZ solutions (0.75% w/v) used to prepare films were easy to
216 handle and no heating was required during their dissolution in deionised water. Chitosan solution can

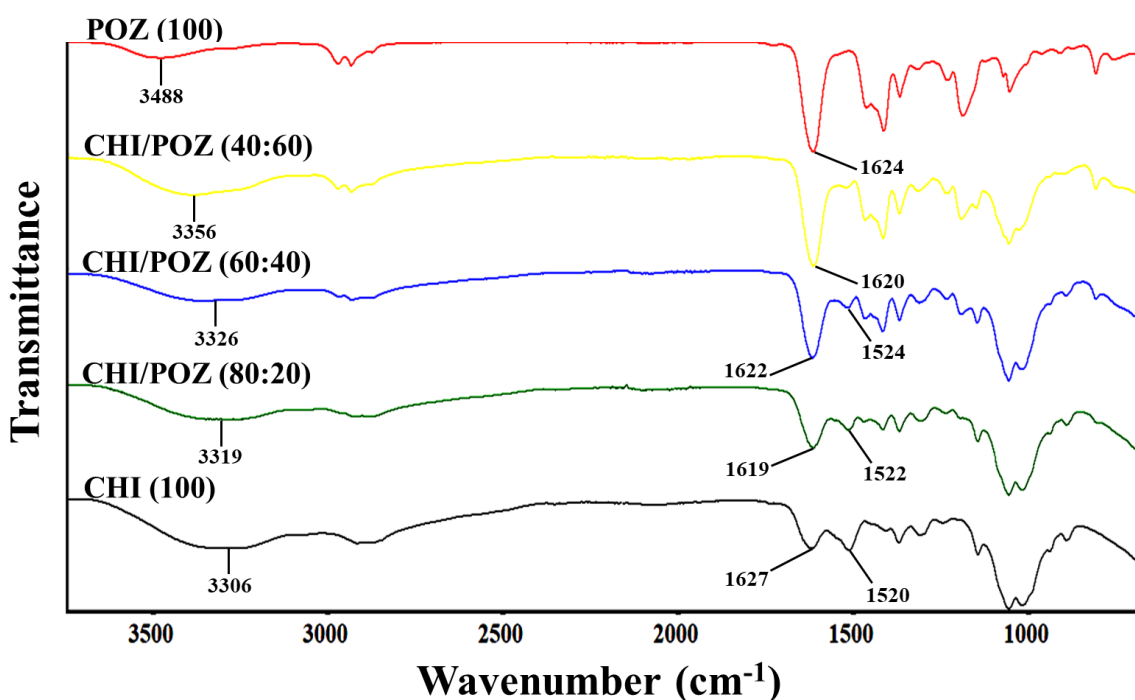
217 be obtained only *via* solvent casting from acidified water. All films were prepared without any
218 plasticisers and were homogenous and transparent.

219 The presence of amide carbonyl groups in poly(2-ethyl-2-oxazoline) suggests that this tertiary
220 polyamide has potential for forming miscible blends with a variety of polymers containing
221 complementary functional groups such as carboxylic, phenolic or alcoholic hydroxyl groups [39–41].
222 Previous studies demonstrated that carbonyl groups of POZ exhibit proton-accepting properties and
223 participate in hydrogen bonding with proton-donating groups of other functional polymers [40,42].
224 Chitosan, in contrast to poly(2-ethyl-2-oxazoline), has in its structure numerous hydroxyl groups that
225 can act as proton-donors with respect to the proton-accepting groups of POZ and form intermolecular
226 hydrogen bonds. In order to establish the possibility of hydrogen bonding in chitosan/POZ blends all
227 films were studied using FTIR spectroscopy (Figure 1). The FTIR spectrum of pure CHI film shows
228 the presence of the broad peak appeared above 3000 cm^{-1} that is due to OH- stretching, which overlaps
229 with NH-stretching in the same region. The peaks at 2923 cm^{-1} and 2889 cm^{-1} correspond to CH_2 -
230 and CH- stretching vibrations. The absorption bands at 1627 cm^{-1} and 1520 cm^{-1} are C=O stretching
231 (amide I) and NH-bending (amide II), respectively. The absorption band at 1416 cm^{-1} is attributed to
232 CH- and OH- vibrations [10]. The band that appeared at 1377 cm^{-1} is assigned to the acetamide
233 groups, which demonstrate that chitosan is not totally deacetylated and the peak at 1316 cm^{-1} can be
234 due to C–N stretching (amide III) [43]. According to Bonilla et al [44] the peak at 1250 cm^{-1}
235 corresponds to amino groups. The peak occurred at 1151 cm^{-1} is the anti-symmetric stretching of the
236 C–O–C bridge, 1062 cm^{-1} and 1024 cm^{-1} are the skeletal vibrations involving the C–O stretching,
237 which are characteristics of chitosan polysaccharide structure [45].

238 The FTIR spectrum of POZ shows the presence of the broad absorption peak at 3488 cm^{-1} ,
239 which is an indication of the presence of bound water that was not eliminated from the film
240 completely. The absorption bands at 2977 cm^{-1} and 2939 cm^{-1} correspond to CH_2 -stretching
241 vibrations. The characteristic bands at 1624 cm^{-1} and 1419 cm^{-1} are assigned to C=O stretching (amide
242 I) and CH_3 bending, respectively [22]. The absorption bands at 1470 , 1374 and 1322 cm^{-1} (CH

243 bending) as well as 1237, 1194 and 1061 cm^{-1} (C-C stretching) are in good agreement with FTIR data
244 on POZ reported in the literature [46].

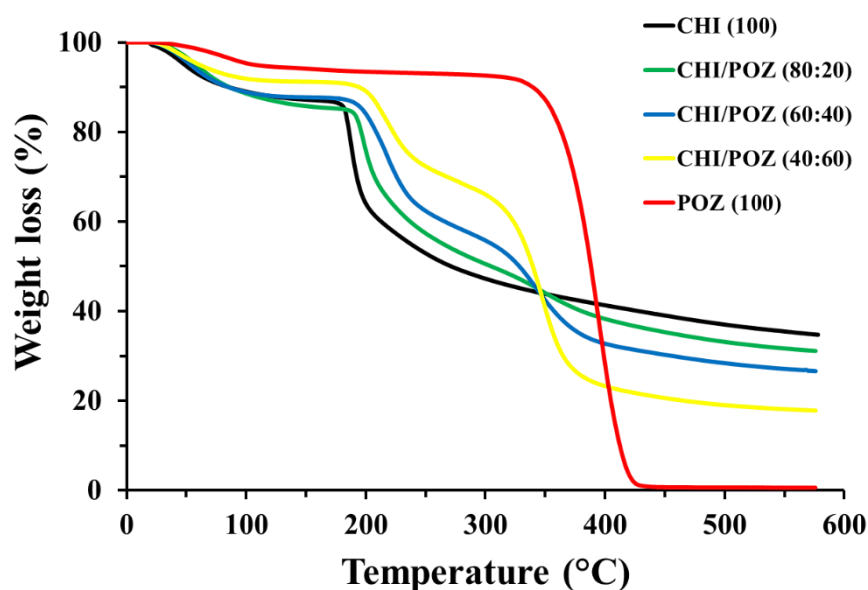
245 All the characteristic bands of the component polymers are present in the spectra of their blends
246 and the intensities of the bands and the shape of the peaks depend on the polymers ratio in the blend.
247 The spectra of the miscible CHI/POZ blends show significant changes in hydroxyl stretching region,
248 suggesting a redistribution in the arrangement of the hydroxyl group associations. When comparing
249 the spectra corresponding to the same system as a function of composition, a shift of this band toward
250 higher wavenumbers is observed for increasing content of POZ. This behaviour suggests that a
251 significant part of the hydroxyl groups involved in CHI are hydrogen-bonded to amide carbonyl
252 groups in POZ. This is in good agreement with the data reported by Fang et al [30].



253
254 **Figure 1.** FTIR spectra of chitosan, POZ and CHI/POZ blends.

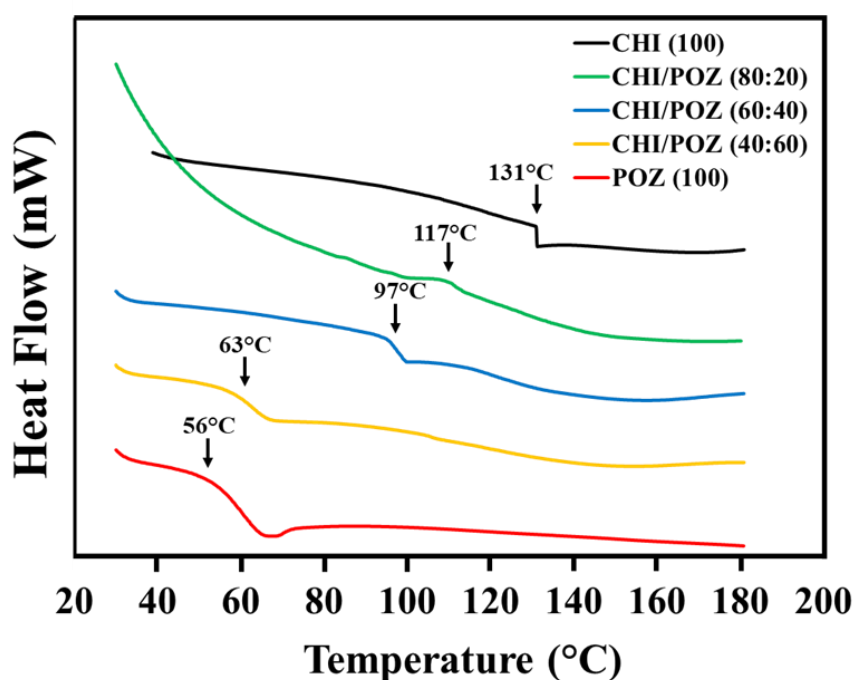
255 Thermogravimetric analysis indicates that degradation of pure chitosan film proceeds via two
256 main stages (Figure 2): first, it starts to loose physically-bound water at $>30\text{ }^{\circ}\text{C}$ and this process
257 finishes at $135\text{ }^{\circ}\text{C}$. The amount of this physically bound water in pure CHI film is about 13 %. The

258 next thermal decomposition stage appears at 178 – 300 °C (with a maximum degradation rate
 259 observed at 188 °C); this degradation results in 52% loss of chitosan weight. This is caused by
 260 depolymerisation of chitosan chains and pyranose rings through dehydration and deamination and
 261 finally ring-opening reaction [47,48]. The pure POZ film shows greater thermal stability compared
 262 to 100 % CHI: the first thermal event begins above 30 °C, which is related to the evaporation of
 263 physically-bound water (approximately 8%). The second stage of thermal decomposition of POZ
 264 starts above 315 °C (with the maximal degradation rate observed at 395 °C) reaching 92% of the total
 265 weight loss at 430 °C. A single decomposition stage of dry POZ at 400 °C was previously reported
 266 by Beruhil Adatoz et al [49], which broadly agrees with our data. The decomposition profiles of
 267 CHI/POZ blends are characterised by three stages: (1) 25 – 150 °C, corresponding to the loss of
 268 physically bound water, (2) 175 – 275 °C, corresponding to the degradation of CHI, and (3) 275 –
 269 425 °C, corresponding to the degradation of POZ. It should be noted that the temperatures, at which
 270 the degradation rates of stages (2) and (3) were maximal, showed a good correlation with the
 271 composition of the blends (Figure S2, Supplementary information). This indicates that the presence
 272 of more thermally stable POZ in the blend improves the thermal stability of less stable chitosan, which
 273 may be due to the presence of weak hydrogen bonding between these polymers.



274
 275 **Figure 2.** TGA curves of pure CHI, pure POZ and CHI/POZ blend films.

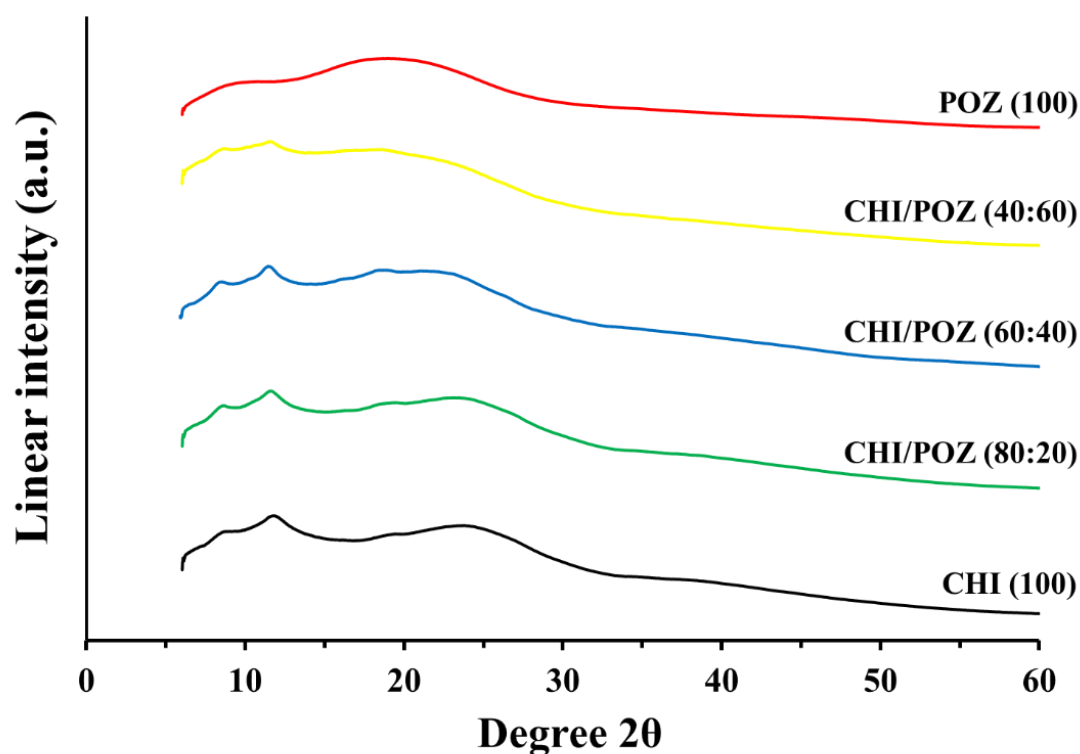
276 Differential scanning calorimetry (DSC) was used to characterize the miscibility between the
 277 polymers. Usually the presence of a single glass transition temperature, situated between T_g values
 278 of individual polymer components indicates a complete miscibility. Figure 3 shows that the presence
 279 of a single glass transition in the blends, which depends on the composition of the polymer mixture.
 280 All glass transition temperatures of the blends are between the T_g values of individual POZ (56 °C)
 281 and chitosan (131 °C), which is in good agreement with the data reported by Fang et al [30].



282
 283 **Figure 3.** DSC thermograms of pure CHI, pure POZ and CHI/POZ blend films.

284 X-ray diffraction (WAXD) method was used to probe the effect of blending on crystallinity of
 285 polymers (Figure 4). WAXD diffractograms of pure CHI and POZ films show a broad halo typical
 286 for predominantly amorphous polymers. Pure CHI still shows the presence of four diffraction peaks
 287 at $2\theta = 8.5^\circ$; 11.8° ; 18.1° and 23.8° , which is typical for crystalline domains in this polysaccharide
 288 and is consistent with our previous report [50]. The diffractogram of pure POZ film shows the
 289 presence of two broad amorphous humps centred at $2\theta = 10.4^\circ$ and 18.8° , indicating non-crystalline
 290 nature of this polymer, which is also consistent with the literature data [51,52].

291 Diffraction peaks characteristic of chitosan are also present in the blend film, however a shift
 292 of a broad diffraction peak from 23.3° to 19.2° is observed. This may indicate that chitosan is involved
 293 in some weak interaction with POZ that affects the formation and structure of its crystalline domains.



294
 295 **Figure. 4.** WAXD diffractograms of CHI and CHI/POZ blend films.

296 The morphology of the polymer film cross-sections and surface were studied by scanning
 297 electron microscope (SEM). The investigation of the sample cross-sections at high magnification
 298 (2000×) reveals that the films have fully homogeneous structure with no signs of phase separation
 299 and interface boundaries (Figure 5). Thus, the SEM data provides another evidence for miscibility
 300 between CHI and POZ in the solid state at different ratios.

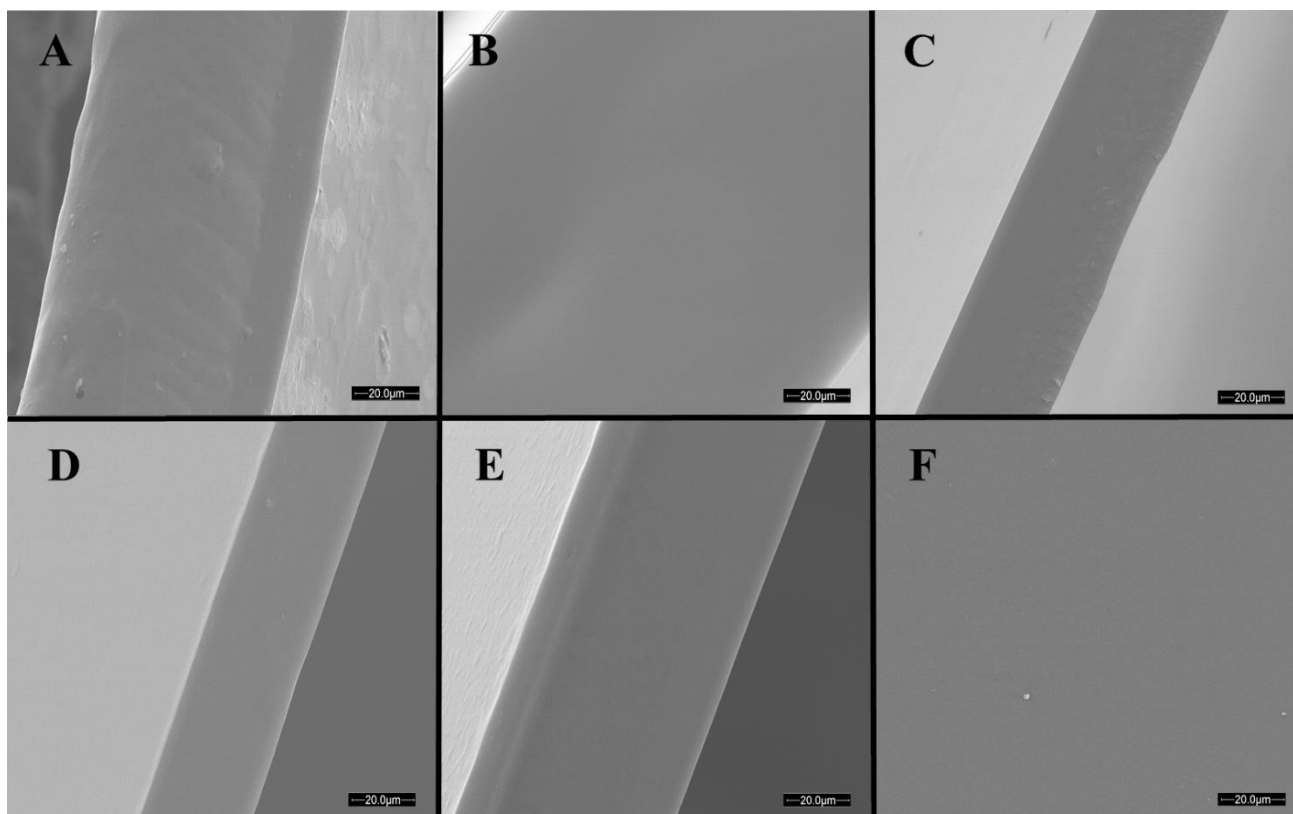


Figure 5. SEM images of (A) CHI, (B) pure POZ, and their blend (C, D, E) cross- sections and (F) surface. Content of POZ in the blends: 20 (C), 40 (D) and 60 % (E, F). Scale bars are 20 μm .

The films composed of the blends with different CHI and POZ ratios were examined by elongation and puncture strength analysis and the results are shown in Figure 6. A film composed of pure POZ was not suitable for this type of analysis because of its extreme brittleness. Comparing the mechanical properties of pure CHI films with the polymer blends indicates that an increase in POZ content in the sample results in gradual reduction in the elongation at break and puncture strength values.

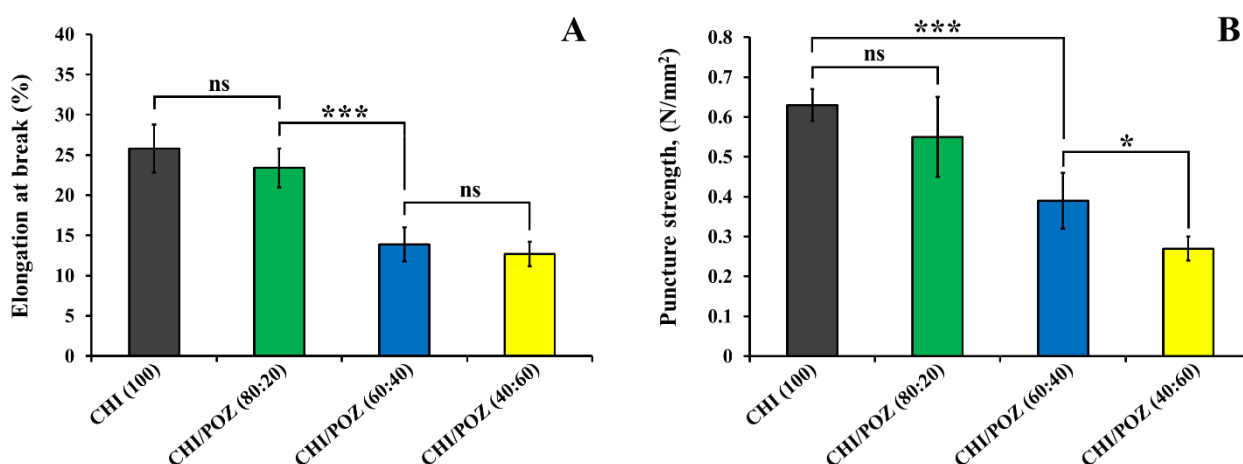


Figure 6. Mechanical analysis of CHI and CHI/POZ blend films: elongation at break (A) and puncture strength (B). Data are expressed as mean \pm standard deviation ($n = 5$). Statistically significant differences are given as: *** – $p < 0.001$; * – $p < 0.05$; ns – no significance.

3.2. Mucosal retention of blend films on *ex vivo* corneal tissue

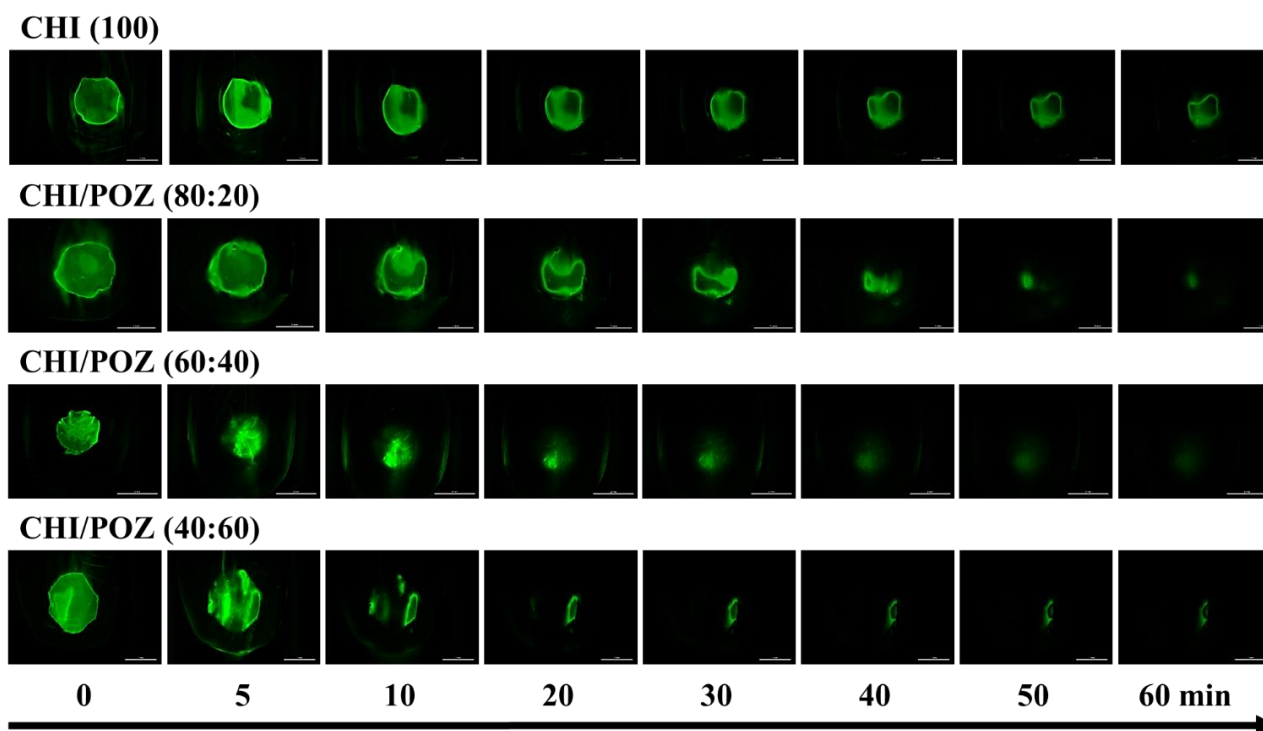
Soluble or swellable polymeric films have been used in ocular therapeutics either to improve the efficiency of drug delivery (compared to conventional eye drops), or to protect the injured cornea [53–55]. These films should exhibit some mucoadhesive properties to have a prolonged residence on the mucosa; however, eventually these materials are supposed to dissolve in the tear fluid completely or should allow their non-traumatising detachment from the ocular surface. These dosage forms should have excellent mechanical properties and a balanced mucoadhesiveness. Materials with insufficiently mucoadhesive properties will not be suitable because of the difficulties in their attachment to the ocular surface and, on the contrary, excessively films will cause discomfort because they may interfere with blinking [56]. Chitosan has previously been reported as a potential material for preparation of mucoadhesive ocular films [57–60]. It exhibits superior mucoadhesive properties compared to many other pharmaceutical polymers, which often needs to be moderated to make it suitable for a particular application. In the present work we have evaluated the suitability of CHI/POZ blends as materials for application as mucoadhesive ocular films.

Fluorescein sodium (NaFl) was used as a model drug to demonstrate the potential use of

CHI/POZ films for the application in ocular drug delivery. The retention of CHI and CHI/POZ films containing 0.1% NaFl on freshly isolated bovine cornea was assessed using a flow-through *in vitro* technique with fluorescent detection. This methodology has been previously used to study the retention of various materials on different mucosal surfaces, including ocular tissues, and it was validated against the other techniques established in assessment of mucoadhesive properties [35,36,38,61,62]. Figure 7 illustrates exemplary fluorescent images of the retention of polymeric films on bovine corneal mucosa irrigated with STF (200 μ L/min). The fluorescence intensity on the mucosa was monitored following each washing cycle over 60 min. After analysing the fluorescent images using ImageJ software, it can be seen that CHI and CHI/POZ films showed an initial increase in fluorescence intensity after the first wash (Figure 8). This can potentially be related to the moisture effect on fluorescent films, causing an increased brightness that leads to >100% fluorescence intensity values. Despite of this initial increase in the fluorescence intensity, the subsequent washes resulted in the reduction of fluorescence intensity due to the dissolution of the films and subsequent wash out of NaFl. It was established that 100% CHI and CHI/POZ (80:20 and 60:40) exhibited significantly greater retention ($p < 0.01$) in the initial washing cycles (except for CHI after 60 min washing, 12 mL STF, $p < 0.05$) compared to CHI/POZ (40:60). It could be concluded that introduction of POZ made the films less retentive. This observation is consistent with our previous studies reporting that decorating nanoparticles with POZ makes them less mucoadhesive [22–24]. Moreover, the retention of CHI/POZ films (80:20 and 60:40) on ocular mucosa was found not to be significantly different from CHI ($p > 0.05$) demonstrating a similar retention profile until the end of washing cycles (Figure 8).

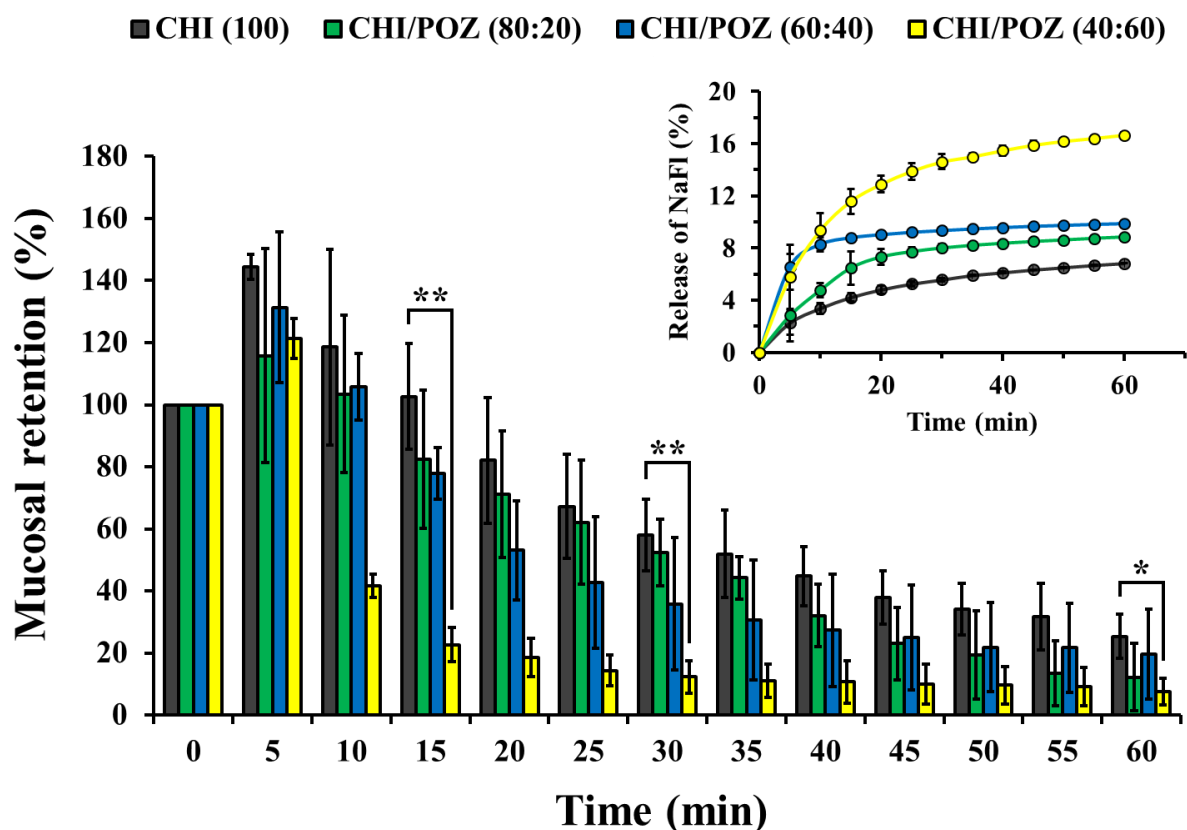
In parallel, STF solution flowing down the corneal surface during each washing cycle was collected at pre-determined time intervals and analysed using fluorescent spectrometry. An insert in Figure 8 depicts the cumulative percentage release of fluorescein sodium from CHI and CHI/POZ films. It was revealed that CHI/POZ (40:60) films released the highest amount of NaFl after total washing cycle over 60 min compared to 100% CHI and CHI/POZ (80:20 and 60:40). In the course

355 of work, the use of NaFl with the concentration higher than 0.1 mg/mL led to the formation of strong
 356 complexes with chitosan and precipitation of complexes were observed. Fluorescein sodium is a
 357 negatively charged compound and therefore may form complexes with the positively charged
 358 backbones of chitosan due to the electrostatic attraction forces. Hence, NaFl with lower concentration
 359 was used to prepare fluorescent films based on different ratios of CHI and POZ. Considering the
 360 composition of CHI/POZ fluorescent films, therefore, the lower content of chitosan in the blend film,
 361 the more NaFl is released. The fact that 100% CHI released less NaFl could be explained by partial
 362 entrapment of fluorescein sodium within the corneal epithelium, or/and by mucoadhesive effects of
 363 chitosan, i.e. specific interactions of chitosan macromolecules with the ocular surface.



364

365 **Figure 7.** Exemplary fluorescent microphotographs showing mucosal retention of CHI and CHI/POZ
 366 films on freshly excised bovine cornea washed with different volumes of STF (200 µL/min) over 60
 367 min. Scale bars are 1 µm.



368

369 **Figure 8.** Mucosal retention of CHI and CHI/POZ films on fresh bovine cornea after irrigating with
 370 different volumes of STF (200 μ L/min) over 60 min. All values are the means \pm standard deviations
 371 of triplicate experiments. Statistically significant differences are given as: ** – $p < 0.01$; * – $p < 0.05$.

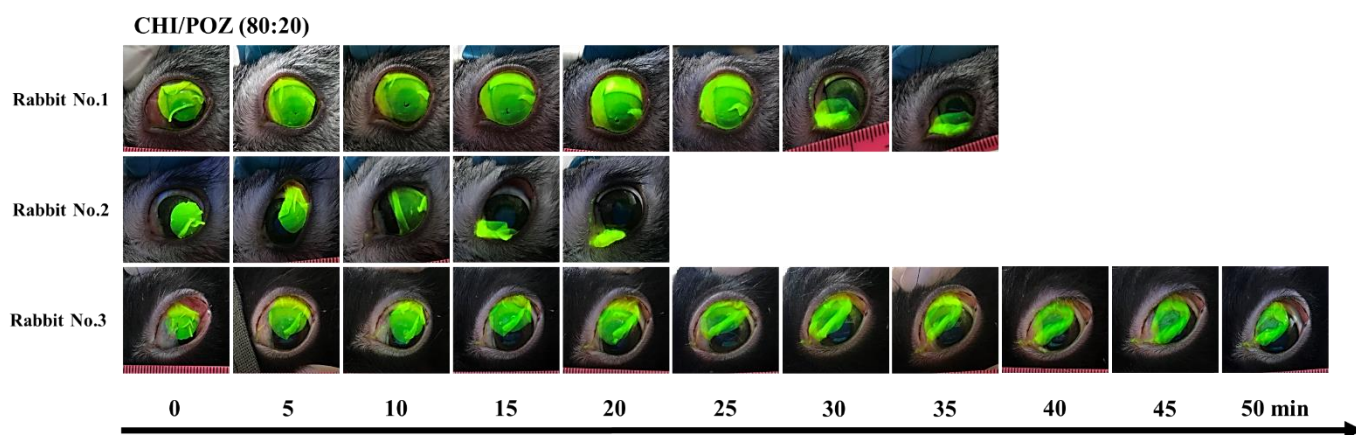
372 3.3. *In vivo* retention studies

373 Taking into consideration the known non-toxic and non-irritant nature of both chitosan and
 374 POZ [14,63] the mucoadhesive films were tested directly *in vivo* without prior evaluation of their
 375 biocompatibility in cell culture or other *in vitro* irritation models.

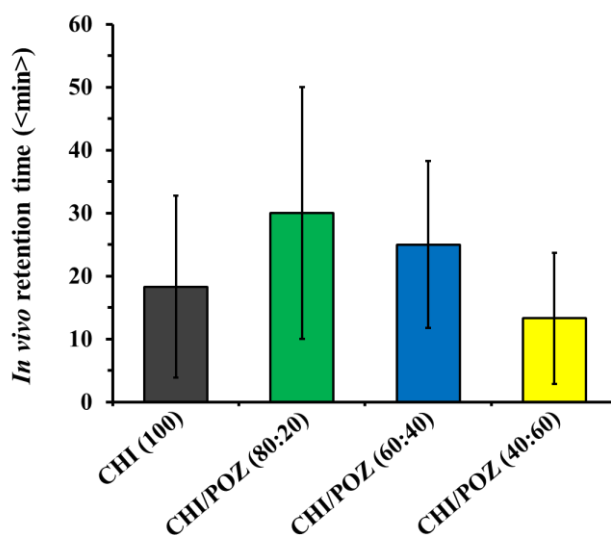
376 *In vivo* experiments were carried out in rabbits ($n = 3$) with round-shaped 10 mm CHI and
 377 CHI/POZ films containing 0.1 mg/mL NaFl. Each formulation was placed on corneal mucosa of a
 378 chinchilla rabbit's left eye and their retention was monitored visually by taking photographs at regular
 379 time points until the films detached. A UV lamp was used to enhance the detection of fluorescence.

380 Figure 9 shows exemplary images of rabbit eyes with fluorescent films administered *in vivo*
 381 providing even coverage of the cornea and subsequent changes were observed, i.e. time of

382 detachment, physical changes such as films swelling and wrinkling. The results for all other
 383 formulations are presented in Figures S3-S6 (Supplementary information). Films made of 100% POZ
 384 were not suitable for *in vivo* experiments due to their extreme brittleness. The *in vivo* results indicate
 385 that pure CHI and CHI/POZ films could achieve from at least 10 min to up to 50 min residence on
 386 the ocular surface, which is consistent with *in vitro* data. Generally, all the films exhibited excellent
 387 adhesion to the cornea. However, the presence of a nictitating membrane on chinchilla rabbit cornea
 388 often led to the dislodging or a complete removal of the films from the corneal surface into the lower
 389 fornix of conjunctiva. This greatly affected *in vivo* data reproducibility. No significant differences (p
 390 > 0.05) were observed between all film formulations in terms of their retention on the rabbit's cornea
 391 (Figure 10). It is expected that these films will exhibit much better retention in human tests because
 392 these dosage forms will not be voluntarily dislodged or removed. It should also be noted that the films
 393 did not cause any observable discomfort, irritation, inflammatory reactions or excessive tear
 394 production in rabbit eyes, which indicate that these materials are biocompatible and potentially
 395 suitable for ocular administration.



396
 397 **Figure 9.** Exemplary photographs of *in vivo* mucosal retention of CHI/POZ (80:20) films on rabbit
 398 eyes taken at different time intervals.



399

400 **Figure 10.** *In vivo* mucosal retention of CHI and CHI/POZ blend films on rabbit eye. Data are
 401 expressed as mean \pm standard deviation (n = 3).

402 4. CONCLUSIONS

403 Polymeric blends of chitosan and poly(2-ethyl-2-oxazoline) were prepared in the form of
 404 flexible and transparent films using casting from aqueous solutions with subsequent solvent
 405 evaporation. The structure and physicochemical properties of these films were evaluated using
 406 Fourier-transformed infrared spectroscopy, thermal gravimetric analysis, differential scanning
 407 calorimetry, wide angle x-ray diffraction, tensile testing and scanning electron microscopy. These
 408 studies indicated a complete miscibility between the polymers in the blends. Blending of chitosan and
 409 poly(2-ethyl-2-oxazoline) leads to a significant reduction of the films mechanical properties
 410 (elongation at break and puncture strength). The films based on pure chitosan and blends with poly(2-
 411 ethyl-2-oxazoline) were formulated with sodium fluorescein and evaluated as potential dosage forms
 412 for ocular drug delivery both *in vitro* and *in vivo*. The results indicate that these films are
 413 biocompatible and do not cause any irritation to the eye. They also exhibit ability to adhere to the
 414 cornea and to retain for up to 50 min, providing a sustained drug release.

415 **ACKNOWLEDGEMENTS**

416 Chemical Analysis Facility (University of Reading) is thanked for providing access to DSC,
417 SEM, TGA and PXRD instruments. The authors are grateful to Amanpreet Kaur and Nick Spencer
418 (University of Reading) for their help with scanning electron microscopy and X-ray diffraction
419 experiments, respectively. G.K.A. acknowledges Ministry of Education and Science of the Republic
420 of Kazakhstan for the research grant (No. AP05133221). D.B.K. gratefully acknowledges the British
421 Council Newton–Al-Farabi Partnership Programme, the Researcher Links Post-Doctoral Mobility
422 Grant (No. 216046068) for financial support of his 2-years of postdoctoral fellowship at the
423 University of Reading. P.C. Turner Abattoirs (Farnborough, United Kingdom) is also thanked for
424 providing bovine eye tissues for experiments. The authors are grateful to Shariat Bolatova (Semey
425 State Medical University, Kazakhstan) for her technical assistance with *in vivo* experiments.

426 **DATA AVAILABILITY AND SUPPLEMENTARY INFORMATION**

427 The Supplementary Information is available free of charge in PDF format. It contains a standard
428 curve used to determine the amount of freed fluorescein sodium from CHI and CHI/POZ films (Figure
429 S1); correlation between the maximal decomposition rate temperature and composition of polymer
430 blends (Figure S2); and exemplary photographs of *in vivo* mucosal retention of CHI and CHI/POZ
431 films on rabbit eyes taken at different time points (Figure S3-S6).

432 **ABBREVIATIONS**

433 CHI, chitosan; DSC, differential scanning calorimetry; EB, elongation at break; PBS, phosphate
434 buffered saline; POZ, poly(2-ethyl-2-oxazoline); PS, puncture strength; SEM, scanning electron
435 microscope; STF, simulated tear fluid; NaFl, fluorescein sodium salt; TGA, thermogravimetric
436 analysis; WAXD, wide-angle X-Ray diffraction.

437 **Author contributions**

438 The manuscript was written through contributions of all authors. All authors have given
439 approval to the final version of the manuscript.

440 **Notes**

441 The authors declare no competing financial interest.

442 **ORCID ID of authors**

443 **Daulet B. Kaldybekov:** <https://orcid.org/0000-0002-7191-5465>

444 **Aisulu Zh. Saimova:** <https://orcid.org/0000-0002-9564-732X>

445 **Galiya S. Irmukhametova:** <https://orcid.org/0000-0002-1264-7974>

446 **Vitaliy V. Khutoryanskiy:** <https://orcid.org/0000-0002-7221-2630>

447 **REFERENCES**

- 448 [1] G.P. Andrews, T.P. Lavery, D.S. Jones, Mucoadhesive polymeric platforms for controlled
449 drug delivery, Eur. J. Pharm. Biopharm. 71 (2009) 505–518.
450 doi:<https://doi.org/10.1016/j.ejpb.2008.09.028>.
- 451 [2] V. V. Khutoryanskiy, Advances in mucoadhesion and mucoadhesive polymers, Macromol.
452 Biosci. 11 (2011) 748–764. doi:10.1002/mabi.201000388.
- 453 [3] V. V. Khutoryanskiy, Mucoadhesive Materials and Drug Delivery Systems, John Wiley &
454 Sons, Ltd, Chichester, UK, 2014. doi:10.1002/9781118794203.
- 455 [4] S. Mansuri, P. Kesharwani, K. Jain, R.K. Tekade, N.K. Jain, Mucoadhesion: A promising
456 approach in drug delivery system, React. Funct. Polym. 100 (2016) 151–172.
457 doi:<https://doi.org/10.1016/j.reactfunctpolym.2016.01.011>.
- 458 [5] A.R. Mackie, F.M. Goycoolea, B. Menchicchi, C.M. Caramella, F. Saporito, S. Lee, K.
459 Stephansen, I.S. Chronakis, M. Hiorth, M. Adamczak, M. Waldner, H. Mørck Nielsen, L.

- 460 Marcelloni, Innovative methods and applications in mucoadhesion research, *Macromol.*
 461 *Biosci.* 17 (2017) 1600534. doi:10.1002/mabi.201600534.
- 462 [6] M. Amidi, E. Mastrobattista, W. Jiskoot, W.E. Hennink, Chitosan-based delivery systems for
 463 protein therapeutics and antigens, *Adv. Drug Deliv. Rev.* 62 (2010) 59–82.
 464 doi:https://doi.org/10.1016/j.addr.2009.11.009.
- 465 [7] A. Bernkop-Schnürch, S. Dünnhaupt, Chitosan-based drug delivery systems, *Eur. J. Pharm.*
 466 *Biopharm.* 81 (2012) 463–469. doi:https://doi.org/10.1016/j.ejpb.2012.04.007.
- 467 [8] L. Casettari, L. Illum, Chitosan in nasal delivery systems for therapeutic drugs, *J. Control.*
 468 *Release.* 190 (2014) 189–200. doi:https://doi.org/10.1016/j.jconrel.2014.05.003.
- 469 [9] T.M.M. Ways, W.M. Lau, V. V Khutoryanskiy, Chitosan and its derivatives for application
 470 in mucoadhesive drug delivery systems, *Polymers (Basel)*. 10 (2018) 267–304.
 471 doi:10.3390/polym10030267.
- 472 [10] K. Luo, J. Yin, O. V Khutoryanskaya, V. V Khutoryanskiy, Mucoadhesive and elastic films
 473 based on blends of chitosan and hydroxyethylcellulose, *Macromol. Biosci.* 8 (2008) 184–
 474 192. doi:10.1002/mabi.200700185.
- 475 [11] M.S. Freag, W.M. Saleh, O.Y. Abdallah, Exploiting polymer blending approach for
 476 fabrication of buccal chitosan-based composite sponges with augmented mucoadhesive
 477 characteristics, *Eur. J. Pharm. Sci.* 120 (2018) 10–19.
 478 doi:https://doi.org/10.1016/j.ejps.2018.04.041.
- 479 [12] R.H. Sizílio, J.G. Galvão, G.G.G. Trindade, L.T.S. Pina, L.N. Andrade, J.K.M.C. Gonsalves,
 480 A.A.M. Lira, M. V Chaud, T.F.R. Alves, M.L.P.M. Arguelho, R.S. Nunes, Chitosan/PVP-
 481 based mucoadhesive membranes as a promising delivery system of betamethasone-17-
 482 valerate for aphthous stomatitis, *Carbohydr. Polym.* 190 (2018) 339–345.
 483 doi:https://doi.org/10.1016/j.carbpol.2018.02.079.
- 484 [13] R. Hoogenboom, Poly(2-oxazoline)s: A polymer class with numerous potential applications,
 485 *Angew. Chemie Int. Ed.* 48 (2009) 7978–7994. doi:10.1002/anie.200901607.

- 486 [14] R. Luxenhofer, Y. Han, A. Schulz, J. Tong, Z. He, A. V Kabanov, R. Jordan, Poly(2-
487 oxazoline)s as polymer therapeutics, *Macromol. Rapid Commun.* 33 (2012) 1613–1631.
488 doi:10.1002/marc.201200354.
- 489 [15] O. Sedlacek, B.D. Monnery, S.K. Filippov, R. Hoogenboom, M. Hruby, Poly(2-Oxazoline)s
490 – Are they more advantageous for biomedical applications than other polymers?, *Macromol.*
491 *Rapid Commun.* 33 (2012) 1648–1662. doi:10.1002/marc.201200453.
- 492 [16] H. Bludau, A.E. Czapar, A.S. Pitek, S. Shukla, R. Jordan, N.F. Steinmetz, POxylation as an
493 alternative stealth coating for biomedical applications, *Eur. Polym. J.* 88 (2017) 679–688.
494 doi:https://doi.org/10.1016/j.eurpolymj.2016.10.041.
- 495 [17] T. Lorson, M.M. Lübtow, E. Wegener, M.S. Haider, S. Borova, D. Nahm, R. Jordan, M.
496 Sokolski-Papkov, A. V Kabanov, R. Luxenhofer, Poly(2-oxazoline)s based biomaterials: A
497 comprehensive and critical update, *Biomaterials.* 178 (2018) 204–280.
498 doi:https://doi.org/10.1016/j.biomaterials.2018.05.022.
- 499 [18] A. Sundaramurthy, M. Vergaelen, S. Maji, R. Auzély-Velty, Z. Zhang, B.G. De Geest, R.
500 Hoogenboom, Hydrogen bonded multilayer films based on poly(2-oxazoline)s and tannic
501 acid, *Adv. Healthc. Mater.* 3 (2014) 2040–2047. doi:10.1002/adhm.201400377.
- 502 [19] S. Hendessi, P.T. Güner, A. Miko, A.L. Demirel, Hydrogen bonded multilayers of poly(2-
503 ethyl-2-oxazoline) stabilized silver nanoparticles and tannic acid, *Eur. Polym. J.* 88 (2017)
504 666–678. doi:https://doi.org/10.1016/j.eurpolymj.2016.10.039.
- 505 [20] C. Su, J. Sun, X. Zhang, D. Shen, S. Yang, Hydrogen-bonded polymer complex thin film of
506 poly(2-oxazoline) and poly(acrylic acid), *Polymers (Basel).* 9 (2017) 363.
507 doi:10.3390/polym9080363.
- 508 [21] R. Hoogenboom, H. Schlaad, Thermoresponsive poly(2-oxazoline)s, polypeptoids, and
509 polypeptides, *Polym. Chem.* 8 (2017) 24–40. doi:10.1039/C6PY01320A.
- 510 [22] E.D.H. Mansfield, K. Sillence, P. Hole, A.C. Williams, V. V Khutoryanskiy, POZylation: a
511 new approach to enhance nanoparticle diffusion through mucosal barriers, *Nanoscale.* 7

512 (2015) 13671–13679. doi:10.1039/C5NR03178H.

513 [23] E.D.H. Mansfield, V.R. de la Rosa, R.M. Kowalczyk, I. Grillo, R. Hoogenboom, K. Sillence,
514 P. Hole, A.C. Williams, V. V Khutoryanskiy, Side chain variations radically alter the
515 diffusion of poly(2-alkyl-2-oxazoline) functionalised nanoparticles through a mucosal
516 barrier, *Biomater. Sci.* 4 (2016) 1318–1327. doi:10.1039/C6BM00375C.

517 [24] T.M.M. Ways, W.M. Lau, K.W. Ng, V. V Khutoryanskiy, Synthesis of thiolated, PEGylated
518 and POZylated silica nanoparticles and evaluation of their retention on rat intestinal mucosa
519 in vitro, *Eur. J. Pharm. Sci.* 122 (2018) 230–238.
520 doi:https://doi.org/10.1016/j.ejps.2018.06.032.

521 [25] L. Ruiz-Rubio, M.L. Alonso, L. Pérez-Álvarez, R.M. Alonso, J.L. Vilas, V. V
522 Khutoryanskiy, Formulation of Carbopol®/Poly(2-ethyl-2-oxazoline)s mucoadhesive tablets
523 for buccal delivery of hydrocortisone, *Polymers (Basel)*. 10 (2018) 175.
524 doi:10.3390/polym10020175.

525 [26] J. Dai, S.H. Goh, S.Y. Lee, K.S. Slow, Complexation between poly(2-hydroxypropyl
526 methacrylate) and three tertiary amide polymers, *J. Appl. Polym. Sci.* 53 (1994) 837–845.
527 doi:10.1002/app.1994.070530701.

528 [27] J. Dai, S.H. Goh, S.Y. Lee, K.S. Siow, Miscibility and interpolymer complexation of poly(2-
529 methyl-2-oxazoline) with hydroxyl-containing polymers, *J. Polym. Res.* 2 (1995) 209–215.
530 doi:10.1007/BF01492772.

531 [28] J.R. Isasi, E. Meaurio, C. Cesteros, I. Katime, Miscibility and specific interactions in blends
532 of poly(2-ethyl-2-oxazoline) with hydroxylated polymethacrylates, *Macromol. Chem. Phys.*
533 197 (1996) 641–649. doi:10.1002/macp.1996.021970219.

534 [29] S. Kobayashi, M. Kaku, T. Saegusa, Miscibility of poly(2-oxazolines) with commodity
535 polymers, *Macromolecules*. 21 (1988) 334–338. doi:10.1021/ma00180a009.

536 [30] L. Fang, S.H. Goh, Miscible chitosan/tertiary amide polymer blends, *J. Appl. Polym. Sci.* 76
537 (2000) 1785–1790. doi:10.1002/(SICI)1097-4628(20000620)76:12<1785::AID-

538 APP8>3.0.CO;2-B.

539 [31] P.J.A. Sobral, F.C. Menegalli, M.D. Hubinger, M.A. Roques, Mechanical, water vapor
540 barrier and thermal properties of gelatin based edible films, *Food Hydrocoll.* 15 (2001) 423–
541 432. doi:10.1016/S0268-005X(01)00061-3.

542 [32] S. Mali, M.V.E. Grossmann, M.A. García, M.N. Martino, N.E. Zaritzky, Barrier, mechanical
543 and optical properties of plasticized yam starch films, *Carbohydr. Polym.* 56 (2004) 129–
544 135. doi:10.1016/j.carbpol.2004.01.004.

545 [33] M. Preis, K. Knop, J. Breitzkreutz, Mechanical strength test for orodispersible and buccal
546 films, *Int. J. Pharm.* 461 (2014) 22–29. doi:10.1016/J.IJPHARM.2013.11.033.

547 [34] R. Gnanasambandam, N.S. Hettiarachchy, M. Coleman, Mechanical and barrier properties of
548 rice bran films, *J. Food Sci.* 62 (1997) 395–398. doi:10.1111/j.1365-2621.1997.tb04009.x.

549 [35] G.S. Irmukhametova, G.A. Mun, V. V Khutoryanskiy, Thiolated mucoadhesive and
550 PEGylated nonmucoadhesive organosilica nanoparticles from 3-
551 mercaptopropyltrimethoxysilane, *Langmuir.* 27 (2011) 9551–9556. doi:10.1021/la201385h.

552 [36] E.A. Mun, P.W.J. Morrison, A.C. Williams, V. V Khutoryanskiy, On the barrier properties of
553 the cornea: A microscopy study of the penetration of fluorescently labeled nanoparticles,
554 polymers, and sodium fluorescein, *Mol. Pharm.* 11 (2014) 3556–3564.
555 doi:10.1021/mp500332m.

556 [37] P.W.J. Morrison, N.N. Porfiryeva, S. Chahal, I.A. Salakhov, C. Lacourt, I.I. Semina, R.I.
557 Moustafine, V. V Khutoryanskiy, Crown ethers: Novel permeability enhancers for ocular
558 drug delivery?, *Mol. Pharm.* 14 (2017) 3528–3538.
559 doi:10.1021/acs.molpharmaceut.7b00556.

560 [38] K. Al Khateb, E.K. Ozhmukhametova, M.N. Mussin, S.K. Seilkhanov, T.K. Rakhypbekov,
561 W.M. Lau, V. V Khutoryanskiy, In situ gelling systems based on Pluronic F127/Pluronic F68
562 formulations for ocular drug delivery, *Int. J. Pharm.* 502 (2016) 70–79.
563 doi:10.1016/j.ijpharm.2016.02.027.

- 564 [39] E. Meaurio, L. Cesteros, L.G. Parada, I. Katime, Blends of poly(mono N-alkyl itaconates)
565 with tertiary polyamides: Specific interactions and thermal degradation, *Polym. J.* 36 (2004)
566 84–90. doi:10.1295/polymj.36.84.
- 567 [40] L.G. Parada, E. Meaurio, L.C. Cesteros, I. Katime, Miscibility behaviour in blends of
568 copolymers of vinyl alcohol with poly(ethyl-oxazoline), *Macromol. Chem. Phys.* 199 (1998)
569 1597–1602. doi:10.1002/(SICI)1521-3935(19980801)199:8<1597::AID-
570 MACP1597>3.3.CO;2-W.
- 571 [41] S.H. Goh, S.Y. Lee, X. Zhou, K.L. Tan, Miscibility and specific interactions in two
572 polyelectrolyte/poly(2-ethyl-2-oxazoline) blend systems, *Polymer (Guildf)*. 40 (1999) 2667–
573 2673. doi:10.1016/S0032-3861(98)00501-1.
- 574 [42] M. Maldonado-Santoyo, C. Ortíz-Estrada, G. Luna-Bárcenas, I.C. Sanchez, L.C. Cesteros, I.
575 Katime, S.M. Nuño-Donlucas, Miscibility behavior and hydrogen bonding in blends of
576 poly(vinyl phenyl ketone hydrogenated) and poly(2-ethyl-2-oxazoline), *J. Polym. Sci. Part B*
577 *Polym. Phys.* 42 (2004) 636–645. doi:10.1002/polb.10758.
- 578 [43] I. Leceta, P. Guerrero, I. Ibarburu, M.T. Dueñas, K. de la Caba, Characterization and
579 antimicrobial analysis of chitosan-based films, *J. Food Eng.* 116 (2013) 889–899.
580 doi:https://doi.org/10.1016/j.jfoodeng.2013.01.022.
- 581 [44] J. Bonilla, E. Fortunati, L. Atarés, A. Chiralt, J.M. Kenny, Physical, structural and
582 antimicrobial properties of poly vinyl alcohol–chitosan biodegradable films, *Food Hydrocoll.*
583 35 (2014) 463–470. doi:https://doi.org/10.1016/j.foodhyd.2013.07.002.
- 584 [45] C.L. Silva, J.C. Pereira, A. Ramalho, A.A.C.C. Pais, J.J.S. Sousa, Films based on chitosan
585 polyelectrolyte complexes for skin drug delivery: Development and characterization, *J.*
586 *Memb. Sci.* 320 (2008) 268–279. doi:https://doi.org/10.1016/j.memsci.2008.04.011.
- 587 [46] A. Colombo, F. Gherardi, S. Goidanich, J.K. Delaney, E.R. de la Rie, M.C. Ubaldi, L.
588 Toniolo, R. Simonutti, Highly transparent poly(2-ethyl-2-oxazoline)-TiO₂ nanocomposite
589 coatings for the conservation of matte painted artworks, *RSC Adv.* 5 (2015) 84879–84888.

doi:10.1039/C5RA10895K.

[47] A. Pawlak, M. Mucha, Thermogravimetric and FTIR studies of chitosan blends, *Thermochim. Acta.* 396 (2003) 153–166. doi:[https://doi.org/10.1016/S0040-6031\(02\)00523-3](https://doi.org/10.1016/S0040-6031(02)00523-3).

[48] T. Wanjun, W. Cunxin, C. Donghua, Kinetic studies on the pyrolysis of chitin and chitosan, *Polym. Degrad. Stab.* 87 (2005) 389–394. doi:<https://doi.org/10.1016/j.polymdegradstab.2004.08.006>.

[49] E. Beruhil Adatoz, S. Hendessi, C.W. Ow-Yang, A.L. Demirel, Restructuring of poly(2-ethyl-2-oxazoline)/tannic acid multilayers into fibers, *Soft Matter.* 14 (2018) 3849–3857. doi:10.1039/C8SM00381E.

[50] J. Yin, K. Luo, X. Chen, V. V Khutoryanskiy, Miscibility studies of the blends of chitosan with some cellulose ethers, *Carbohydr. Polym.* 63 (2006) 238–244. doi:10.1016/J.CARBPOL.2005.08.041.

[51] A. Shubha, S.R. Manohara, L. Gerward, Influence of polyvinylpyrrolidone on optical, electrical, and dielectric properties of poly(2-ethyl-2-oxazoline)-polyvinylpyrrolidone blends, *J. Mol. Liq.* 247 (2017) 328–336. doi:<https://doi.org/10.1016/j.molliq.2017.09.086>.

[52] H. Fael, C. Ràfols, A.L. Demirel, Poly(2-ethyl-2-oxazoline) as an alternative to poly(vinylpyrrolidone) in solid dispersions for solubility and dissolution rate enhancement of drugs, *J. Pharm. Sci.* 107 (2018) 2428–2438. doi:<https://doi.org/10.1016/j.xphs.2018.05.015>.

[53] H. Abdelkader, B. Pierscionek, R.G. Alany, Novel in situ gelling ocular films for the opioid growth factor-receptor antagonist-naltrexone hydrochloride: Fabrication, mechanical properties, mucoadhesion, tolerability and stability studies, *Int. J. Pharm.* 477 (2014) 631–642. doi:<https://doi.org/10.1016/j.ijpharm.2014.10.069>.

[54] H.S. Mahajan, S.R. Deshmukh, Development and evaluation of gel-forming ocular films based on xyloglucan, *Carbohydr. Polym.* 122 (2015) 243–247. doi:<https://doi.org/10.1016/j.carbpol.2015.01.018>.

- 616 [55] S. Karki, H. Kim, S.-J. Na, D. Shin, K. Jo, J. Lee, Thin films as an emerging platform for
617 drug delivery, *Asian J. Pharm. Sci.* 11 (2016) 559–574.
618 doi:<https://doi.org/10.1016/j.ajps.2016.05.004>.
- 619 [56] O. V Khutoryanskaya, P.W.J. Morrison, S.K. Seilkhanov, M.N. Mussin, E.K.
620 Ozhmukhametova, T.K. Rakhypbekov, V. V Khutoryanskiy, Hydrogen-bonded complexes
621 and blends of poly(acrylic acid) and methylcellulose: Nanoparticles and mucoadhesive films
622 for ocular delivery of riboflavin, *Macromol. Biosci.* 14 (2014) 225–234.
623 doi:10.1002/mabi.201300313.
- 624 [57] G. de O. Fulgêncio, F.A.B. Viana, R.R. Ribeiro, M.I. Yoshida, A.G. Faraco, A. da S. Cunha-
625 Júnior, New mucoadhesive chitosan film for ophthalmic drug delivery of timolol maleate: In
626 vivo evaluation, *J. Ocul. Pharmacol. Ther.* 28 (2012) 350–358. doi:10.1089/jop.2011.0174.
- 627 [58] R.M.D. Byrro, G. de Oliveira Fulgêncio, A. da Silva Cunha, I.C. César, P.R. Chellini, G.A.
628 Pianetti, Determination of ofloxacin in tear by HPLC–ESI-MS/MS method: Comparison of
629 ophthalmic drug release between a new mucoadhesive chitosan films and a conventional eye
630 drop formulation in rabbit model, *J. Pharm. Biomed. Anal.* 70 (2012) 544–548.
631 doi:<https://doi.org/10.1016/j.jpba.2012.05.003>.
- 632 [59] G. de Oliveira Fulgêncio, F.A.B. Viana, R.O.S. Silva, F.C.F. Lobato, R.R. Ribeiro, J.R.
633 Fanca, R.M.D. Byrro, A.A.G. Faraco, A. da Silva Cunha-Júnior, Mucoadhesive chitosan
634 films as a potential ocular delivery system for ofloxacin: preliminary in vitro studies, *Vet.*
635 *Ophthalmol.* 17 (2014) 150–155. doi:10.1111/vop.12140.
- 636 [60] K. Hermans, D. Van den Plas, S. Kerimova, R. Carleer, P. Adriaenssens, W. Weyenberg, A.
637 Ludwig, Development and characterization of mucoadhesive chitosan films for ophthalmic
638 delivery of cyclosporine A, *Int. J. Pharm.* 472 (2014) 10–19.
639 doi:<https://doi.org/10.1016/j.ijpharm.2014.06.017>.
- 640 [61] P. Tonglairoum, R.P. Brannigan, P. Opanasopit, V. V. Khutoryanskiy, Maleimide-bearing
641 nanogels as novel mucoadhesive materials for drug delivery, *J. Mater. Chem. B.* 4 (2016)

642 6581–6587. doi:10.1039/C6TB02124G.

643 [62] O.M. Kolawole, W.M. Lau, V. V Khutoryanskiy, Chitosan/ β -glycerophosphate in situ
644 gelling mucoadhesive systems for intravesical delivery of mitomycin-C, *Int. J. Pharm.* X. 1
645 (2019) 100007. doi:<https://doi.org/10.1016/j.ijpx.2019.100007>.

646 [63] S. Rodrigues, M. Dionísio, C.R. López, A. Grenha, Biocompatibility of chitosan carriers with
647 application in drug delivery, *J. Funct. Biomater.* 3 (2012). doi:10.3390/jfb3030615.

648